ORIGINAL PAPER

Mechanisms on electrical breakdown strength increment of polyethylene by acetophenone and its analogues addition: a theoretical study

Hui Zhang · Yan Shang · Hong Zhao · Baozhong Han · Zesheng Li

Abstract A theoretical investigation is completed on the mechanism of electrical breakdown strength increment of polyethylene. It is shown that it is one of the most important factors for increasing electrical breakdown strength of polyethylene through keto-enol isomerization of acetophenone and its analogues at the ground state S_0 and the lowest triplet state T_1. The minimum structures and transition states of the keto- and the enol-tautomer of acetophenone and its analogues at the S_0 and T_1 states are obtained at the B3LYP/6-311+ G(d,p) level, as well as the harmonic vibration frequencies of the equilibrium geometries and the minimum energy path (MEP) by the intrinsic reaction coordinate (IRC) theory at the same level. The two C–C bond cleavage reaction channels have been identified in acetophenone. The calculated results show that the energy barriers of keto-enol isomerization of acetophenone and its analogues at S_0 and T_1 states are much

smaller than the average C-C bond energy of polyethylene, and the acetophenone doping or bond linked into polyethylene can increase the electrical breakdown strength and inhibit polyethylene electrical tree initiation and aging.

Keywords Acetophenone · Electrical breakdown strength · Keto-enol isomerization · Polyethylene · Transition state

Introduction

The electrical tree aging is a leading factor of degradation of cross-linking polyethylene (XLPE) insulated high-voltage cable. It limits the life expectancy of the cable insulation and even causes a sudden breakdown of the insulation when the rated voltage is above 110 kV [1–4]. Tu et al. reported the addition in the insulation so called voltage stabilizer that can capture the high mobility electron and absorb the energy accumulated by electrical field. This will cause the 2–4 times increment of initial voltage of electrical tree of XLPE [5]. Yamano et al. and Englund et al. reported that the π-bond of polycyclic aromatic hydrocarbons has the capacity of absorbing the energy of moving electrons. The addition of polycyclic aromatic hydrocarbons is effective for inhibiting the polymer molecule chain fracture caused by electron bombardment, thus increasing the initial voltage of electrical tree of PE and inhibiting the electrical tree initiation [6, 7]. Our research group observed that addition of acetophenone in proper amount leads to a 50 % increase of the alternate current (AC) breakdown strength of PE and a remarkable improvement of electrical tree resistance capability.

The sensitized phosphorescence excitation spectra of jet-cooled acetophenone have been measured by Ito and co-workers [8]. The lowest excited singlet state is S_1 (n, π*) with the origin of S_1 (n, π*) ← S_0 transition of 27 279 cm^{-1} (77.99 kcal mol^{-1}). Additionally, the origin of the first triplet

H. Zhang (✉)
Key Laboratory of Engineering Dielectrics and Its Application of Ministry of Education & College of Chemical and Environmental Engineering, Harbin University of Science and Technology, Harbin 150080, People's Republic of China
e-mail: hust_zhanghui11@hotmail.com

Y. Shang
College of Chemical and Environmental Engineering, Harbin University of Science and Technology, Harbin 150080, People's Republic of China

H. Zhao · B. Han (✉)
Key Laboratory of Engineering Dielectrics and Its Application of Ministry of Education, Harbin University of Science and Technology, Harbin 150080, People's Republic of China
e-mail: hbzhlj@163.com

Z. Li (✉)
Key Laboratory of Cluster Science of Ministry of Education & School of Chemistry, Beijing Institute of Technology, Beijing 100081, People's Republic of China
e-mail: zeshengli@bit.edu.cn

state T_1 (n, $\pi*$) ← S_0 shows at 25 791 cm^{-1} (73.74 kcal mol^{-1}), and the triplet state T_2 (π, $\pi*$) is suggested to lie near T_1 (n, $\pi*$) for the isolated molecule. They raised that the T_2 (π, $\pi*$) triplet state plays an essential role in the efficient S_1-T_2 intersystem crossing. The efficient intersystem crossing from S_1 to the triplet manifold is usually explained by the direct spin-orbit coupling between S_1 and a lower energy T_2. Acetophenone are very weakly fluorescent, but highly phosphorescent under isolated molecular condition.

Fang and co-workers [9, 10] have theoretically discovered a minimum energy crossing point among the three potential energy surfaces (S_1, T_1, and T_2) of acetophenone. The electronic and geometric structures predicted for the transient dark states are in good agreement with those determined using ultrafast electron diffraction experiments by Zewail and co-workers [11, 12]. The existence of the $S_1/T_2/T_1$ intersection results in the S_1 → T_1 transition via the T_2 state. The T_2 state functions as a relay and enables the S_1 → T_1 intersystem crossing to take place with a high rate. This is the reason that the lifetime of S_1 state for aromatic ketones is much shorter than that for aliphatic ketones, and aromatic carbonyl compounds are highly phosphorescent. Therefore C-C bonds cleavage reactions occurs only at the lowest triplet state for most of the aromatic ketones.

Thiel and co-workers [13] reported a theoretical study on the electronic excited states and the mechanisms of photodissociation of acetophenone. They also found the $S_1/T_2/T_1$ three-state intersection which allows for an efficient transition from S_1 to T_1 by intersystem crossing through T_2. Then the radical photodissociation reactions occur in the T_1 state. Excitation (n → $\pi*$) of a ketone from the ground state to its excited state may lead primarily to the cleavage of the α-CC bonds (α-cleavage) at the α position of the excited carbonyl group of carbonyl compounds. This process produces a radical pair (an acyl radical and an alkyl radical). The detailed α-cleavage reaction mechanism and the related dynamic behavior are the key to understanding the photochemistry for the entire carbonyl family. This fundamental photochemical process is commonly known as Norrish type I reaction. Aromatic carbonyl compounds have relatively large π electron conjugation system between the aromatic and carbonyl groups, which influences the photodissociation mechanisms [14, 15]. The T_1 reactions have been identified to mainly yield benzoyl and methyl radicals for acetophenone [16]. The structures of the highest points along the corresponding minimum-energy reaction paths was taken as the transition states for the two C–C bond cleavage reactions.

A spectrum of electronic transitions by symmetry is both spin and orbital forbidden. Such transitions are only allowed through the coupling of nuclear and electronic motions. Spins are singlet-coupled inside chemically stable organic molecules, the ground states of which are spin singlets with closed electronic shells. The first excited states are triplets, since normally such species belong to single electron excitations [17, 18].

Carriers (electrons) which gain enough kinetic energy under the electric field in insulating materials are known as hot electrons. Afterward, bound electrons are knocked free from atoms through the collisions with hot electrons and create new carriers. If this process forms a chain reaction, the carrier concentration in the material will be a sharp increase and it can result in a loss of insulating properties of the material. Hot electrons collide to a special structure molecular (such as acetophenone) and release energy to the molecular in the form of heat energy, then the electrons released from the molecular with low energy are known as secondary electrons. This energy of hot electrons dissipates in three ways when the addition of acetophenone: (1) acetophenone can overcome the barriers then accomplishes isomerization in the ground state S_0; (2) acetophenone can accomplish transitions between different electronic states S_1 (n, $\pi*$) ← S_0 transition; (3) hot electrons hit C-C bond of XLPE and break the bond. When hot electrons are injected into PE composites (include acetophenone as additive), acetophenone will be excited to the first singlet excited state S_1 or higher-lying S_2 state depending on the intensity of the electric voltage. The chemistry process starting from S_2 or S_1 states has been studied very well [8–10]. As introduced above, the molecule will undergo an efficient intersystem crossing from initial excited states to the lowest triplet state T_1 through the $S_1/T_2/T_1$ three-state intersection. These dark intermediate structures and conjectural mechanisms are essential to understanding the mechanism of keto-enol isomerization of acetophenone and play critical roles in PE composites to inhibit polyethylene electrical tree initiation and aging when chemical compound doping or bond linked to PE. However, it is very difficult or impossible to observe the intersection structure involved in the transitions states of acetophenone isomerization on the PE composites in experiments at present. Therefore, the theoretical studies on the keto-enol isomerizations of acetophenone on the ground state and the lowest triplet state are very necessary. It is expected to be informative for understanding the mechanism of electrical breakdown strength increment for polyethylene.

This work aims to provide a systematic study on the mechanism of isomerizations of acetophenone and its analogues at S_0 and T_1 states, and the two C–C bond cleavage reactions occuring in the T_1 state. We focus on the bond cleavage reactions in the lowest triple state, without addressing the competing molecular photodissociation processes [12]. The energy barriers and reaction enthalpies have also been calculated using density function theory [19], involving acetophenone bond linked to the carbon chain of PE (such as structural segments n=1, 2, 3, 4, and 5 versus KCC, p-KP4, p-KP6, p-KP8, and p-KP10, respectively) via para-positions. The different substituent groups, such as alkyl and heteroatoms, have been chosen in the present study to evaluate the substituent and functional effect. A comparison between the theoretical at present and experimental results is discussed.

The research results will be helpful for further experimental investigations. The keto- and enol-tautomers of acetophenone and its analogues are abbreviated to K and E, respectively, while the transition state and reaction channel are abbreviated to TS and R, respectively. For distinguishing the triplet from the singlet state, the "3" is added to the corresponding abbreviations for T_1 state. The two C–C bond cleavage reactions of $C_6H_5COCH_3$ (K) channels in the triplet state are abbreviated to RD1 and RD2. The 30 possible isomerization reaction channels and the two C–C bond cleavage reaction channels have been studied, as follows:

K → E (R)	K3 → E3 (R3)
KC → EC (RC)	KC3 → EC3 (RC3)
KCC → ECC (RCC)	KCC3 → ECC3 (RCC3)
p-KP4 → p-EP4 (p-RP4)	p-KP43 → p-EP43 (p-RP43)
p-KP6 → p-EP6 (p-RP6)	p-KP63 → p-EP63 (p-RP63)
p-KP8 → p-EP8 (p-RP8)	p-KP83 → p-EP83 (p-RP83)
p-KP10 → p-EP10 (p-RP10)	p-KP103 → p-EP103 (p-RP103)
K1 → E1 (R1)	K13 → E13 (R13)
K2 → E2 (R2)	K23 → E23 (R23)
KOH → EOH (ROH)	KOH3 → EOH3 (ROH3)
KOC → EOC (ROC)	KOC3 → EOC3 (ROC3)
KSH → ESH (RSH)	KSH3 → ESH3 (RSH3)
KN → EN (RN)	KN3 → EN3 (RN3)
KNC → ENC (RNC)	KNC3 → ENC3 (RNC3)
KNCOC → ENCOC (RNCOC)	KNCOC3 → ENCOC3 (RNCOC3)
K → C_6H_5CO + CH_3 (RD1)	K → C_6H_5 + $COCH_3$ (RD2)

Computational methods

In the present work, the equilibrium geometries and frequencies of all the stationary points (keto- and enol-tautomers of acetophenone and its analogues, and the corresponding transition states) are optimized at the ground state S_0 and the triplet state T_1 using B3LYP method [20–23] with the 6-311+G(d,p) basis set without any constraint. The minimum energy path (MEP) is obtained by intrinsic reaction coordinate (IRC) theory in mass-weighted Cartesian coordinates with a gradient step-size of 0.05 (amu)$^{1/2}$ bohr. At the same level, the energy derivatives, including gradients and Hessians at geometries along the MEP, are obtained to calculate the curvature of the reaction path and the generalized vibrational frequencies along the reaction path. In order to obtain more accurate energies of the two C–C bond cleavage reactions in acetophenone, the energies of the equilibrium geometries are refined by the quadratic configuration interaction with single and double substitutions with a triple contribution QCISD(T) [24] method based on the B3LYP/6-311+G(d,p) geometries. All the electronic structure calculations are performed using GAUSSIAN09 program package [25].

Results and discussion

Stationary points

The optimized geometric structures on S_0 and T_1 states of the keto tautomers of acetophenone and its analogues, the enol tautomers of acetophenone and its analogues, and the corresponding transition states for 30 reaction channels are completed at the B3LYP/6-311+G(d,p) level, involving the two C–C bond cleavage reactions of acetophenone on T_1 state. The optimized geometric structures of the keto- and enol-tautomers of acetophenone and its analogues, and transition states are presented in Figs. 1, 2, 3. Optimized bond lengths of breaking and forming bonds and the corresponding harmonic vibrational frequencies for the 30 transition states in its S_0 and T_1 states are listed in Table 1 as well as that of the two C–C bond cleavage reactions in T_1 state. All the transition states are confirmed by normal-mode analysis to only have one imaginary frequency corresponding to the stretching modes of the coupling breaking and forming bonds.

In Table 1, it can be seen that the transition state structure on S_0 states TS2 of reaction R2, the length of the O—H bond which will be broken stretches by 35 % over the O—H regular bond length in K2, and the product-forming H—O bond is elongated by about 35 % over the equilibrium bond length in equilibrium E2. Thus, reaction R2 proceeds via a symmetrical barrier. It also can be seen that the other transition state structures of the 30 reactions on S_0 state have a common character. The elongation of the breaking bond is larger than that of the forming bond, the other keto-enol isomerization transition state structures of acetophenone and its analogues reaction systems are all product-like, i.e., those reaction channels will proceed via "late" transition states, which is consistent with Hammond's postulate [26], applied for an endothermic reaction.

Energetics

The reaction enthalpies at 298 K (ΔH_{298}^0) and the potential barrier heights (ΔE^{TS}) with zero-point energy (ZPE) corrections for the 30 reactions calculated at the B3LYP/6-311+G(d,p) level are listed in Table 2, as well as the relative margin of energies (ΔE^{T1-S0}) between S_0 with T_1 states for the keto-tautomers of acetophenone and its analogues, together with that of the two C–C bond cleavage reactions calculated at the QCISD(T)/6-311+G(3df,2p)//B3LYP/6-311+G(d,p) levels (unit in kcal mol^{-1}) in T_1 state. All 30 reactions have energy barriers; especially the reaction enthalpy almost is zero in the T_1 state. As discussed above, the $S_1/T_2/T_1$ three-state intersection region can efficiently funnel electron population from S_1 to T_1 as a consequence of the relay effect of the T_2 state. Therefore we focus on the dissociation reactions in the lowest triplet state. For RD1 and RD2 reactions, the values in
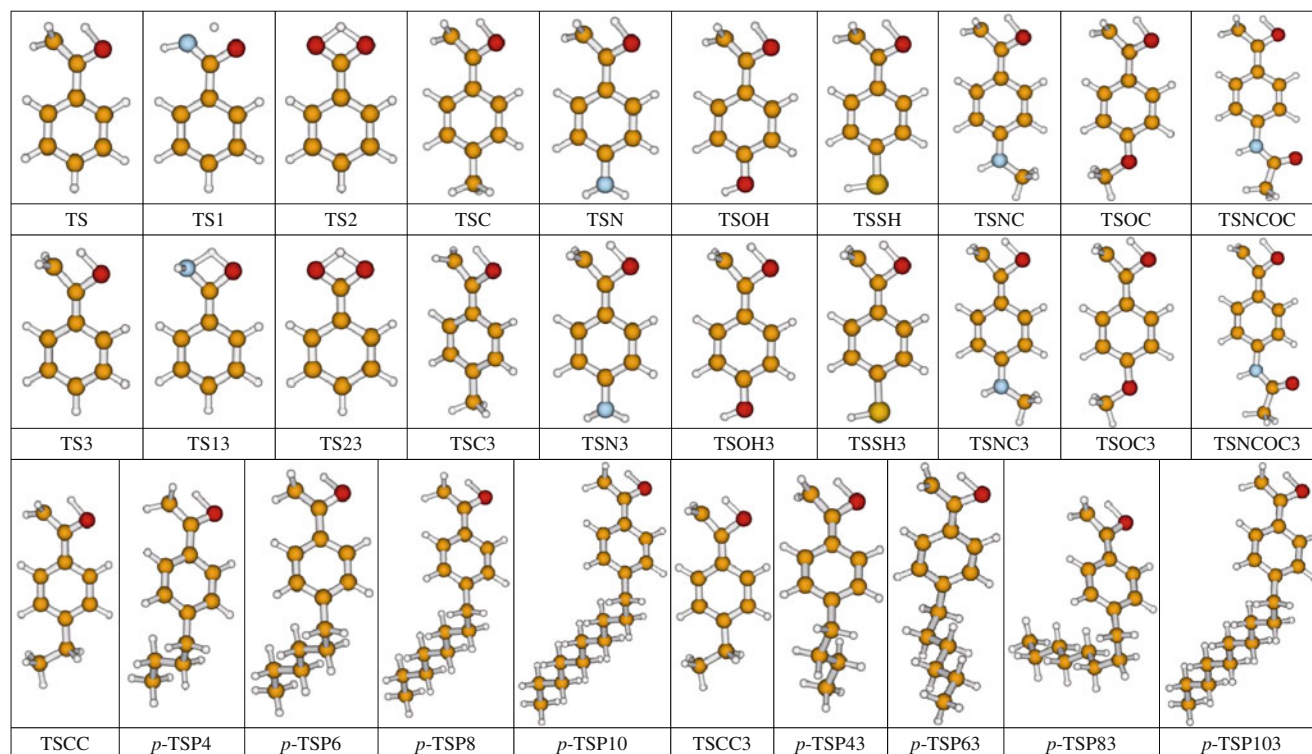
Fig. 1 Optimized geometric structures of the 30 transition states at the B3LYP/6-311+G(d,p) level

parentheses are calculated at the B3LYP/6-311+G(d,p) level. The potential barrier height of reaction channel RD1 (17.92 kcal mol^{-1}) is much lower than the RD2 (27.58 kcal mol^{-1}) at the QCISD(T)//B3LYP level. The former reaction channel (RD1) is less endothermic than the later (RD2) by about 17.19 kcal mol^{-1}, and as a result, RD1 is more
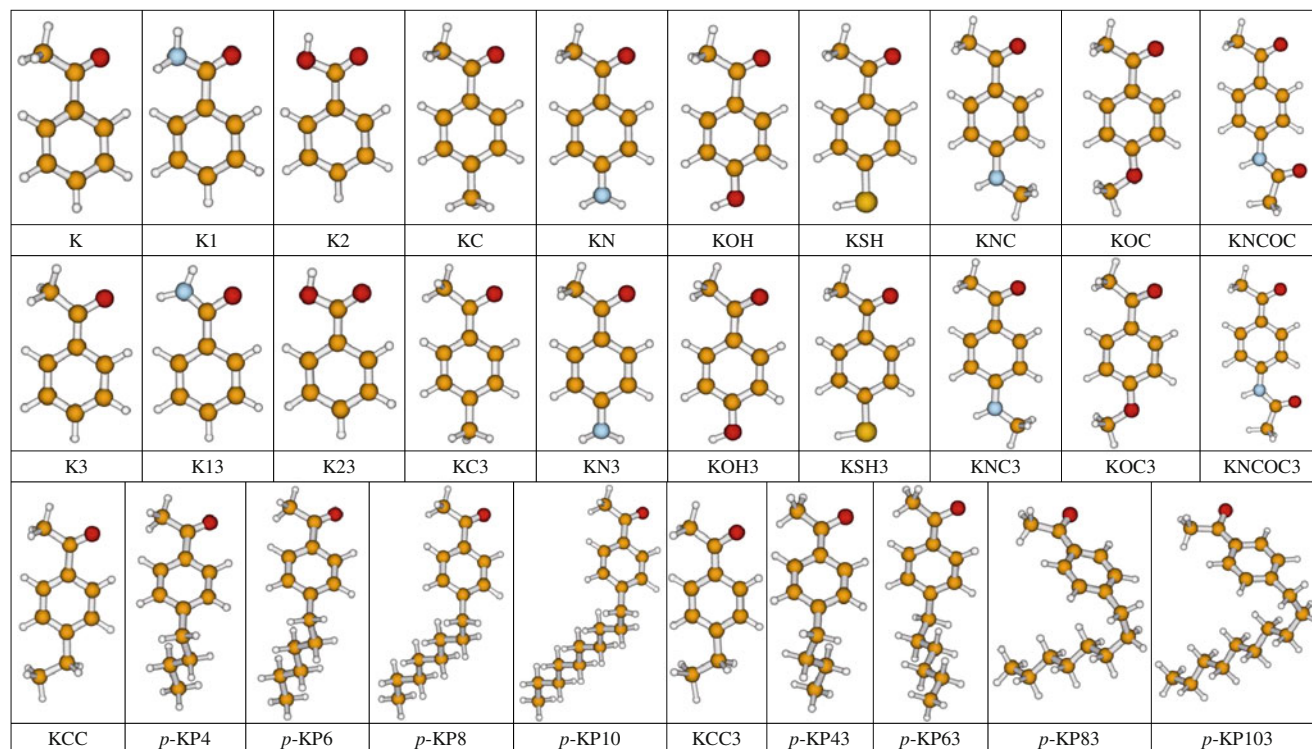

Fig. 2 Optimized geometric structures of the 15 keto tautomer of acetophenone and its analogues at the B3LYP/6-311+G(d,p) level
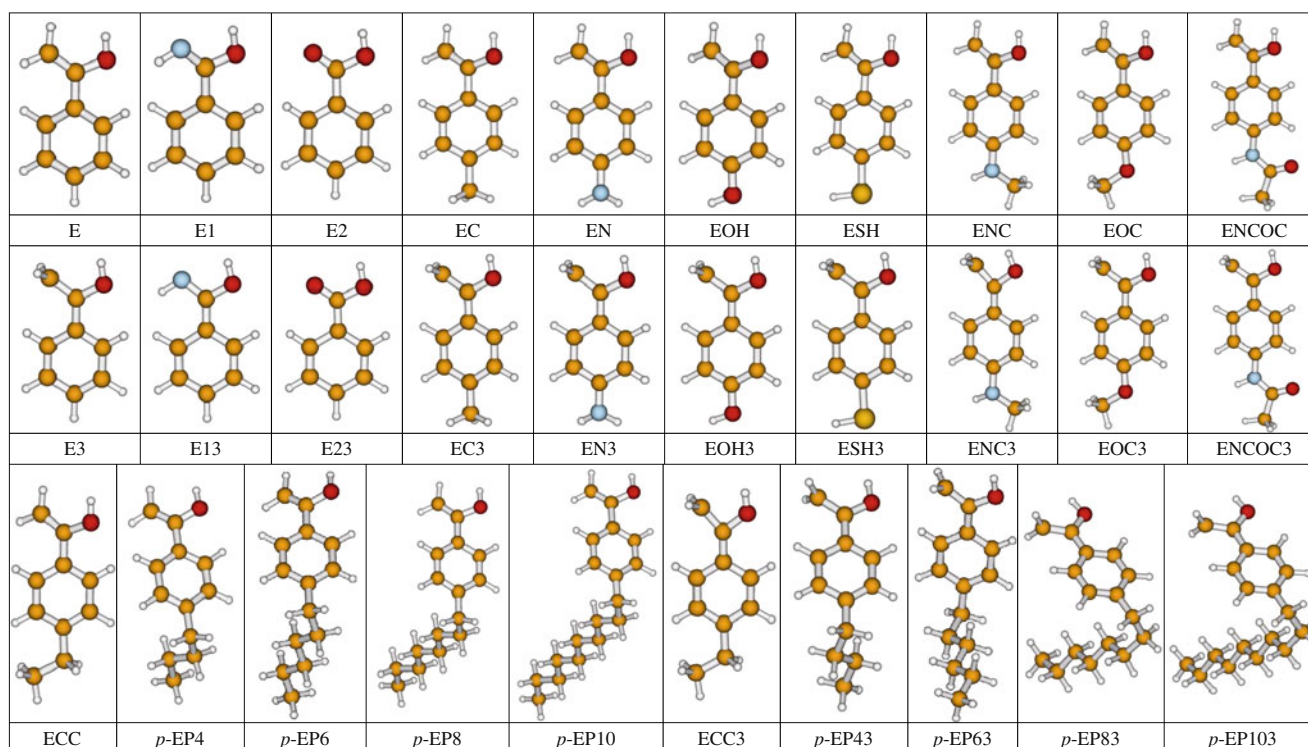
Fig. 3 Optimized geometric structures of the 15 enol tautomer of acetophenone and its analogues at the B3LYP/6-311+G(d,p) level

thermodynamically and kinetically favorable than RD2. The reaction channel RD1 will dominate the formation of ground-state C_6H_5CO and CH_3 radicals, as the products.

Table 3 lists the calculated adiabatic excitation energies of acetophenone in the lowest five electronically excited states
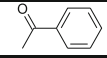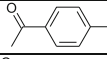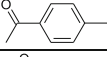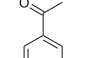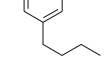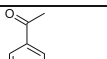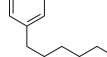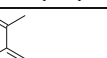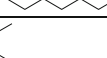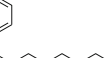
(T_1, S_1, T_2, S_2, and S_3) and the experimental data [8, 10, 12, 13, 27, 28]. The adiabatic excitation energy $\Delta E^{T1\text{-}S0}$ calculated at QCISD(T)//B3LYP level of acetophenone is 74.92 kcal mol^{-1}, showing good consistency with the reported results, 73.74 [8], 73.07 [12], and 72.5 [13] kcal mol^{-1}. This implies

Table 1 Optimized bond lengths of breaking and forming bonds (in angstrom) for the 17 transition states, and calculated frequencies (in cm^{-1}) in its S_0 ground state and T_1 triplet state for the 30 transition states at the B3LYP/6-311+G(d,p) level together with that of the breaking bonds for the two C–C bond cleavage reactions in T_1 state
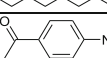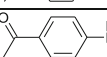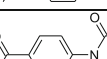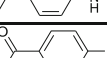
Reaction equation	S_0 (breaking/forming bonds)	S_0 frequencies	T_1 (breaking/forming bonds)	T_1 frequencies
K → E (R)	1.491/1.276	2175 i	1.375/1.281	2004 i
KC → EC (RC)	1.492/1.273	2163 i	1.375/1.281	2004 i
KCC → ECC (RCC)	1.492/1.272	2161 i	1.375/1.282	2004 i
p-KP4 → p-EP4 (p-RP4)	1.492/1.273	2163 i	1.375/1.281	2006 i
p-KP6 → p-EP6 (p-RP6)	1.491/1.274	2166 i	1.374/1.281	2004 i
p-KP8 → p-EP8 (p-RP8)	1.492/1.273	2162 i	1.375/1.281	2005 i
p-KP10 → p-EP10 (p-RP10)	1.493/1.273	2161 i	1.375/1.281	2004 i
K1 → E1 (R1)	1.327/1.316	1956 i	1.304/1.248	2023 i
K2 → E2 (R2)	1.302/1.302	1953 i	1.301/1.301	2038 i
KOH → EOH (ROH)	1.493/1.271	2149 i	1.374/1.282	2004 i
KOC → EOC (ROC)	1.495/1.269	2143 i	1.374/1.282	2004 i
KSH → ESH (RSH)	1.492/1.274	2163 i	1.375/1.282	2003 i
KN → EN (RN)	1.496/1.266	2126 i	1.373/1.282	2004 i
KNC → ENC (RNC)	1.496/1.265	2116 i	1.373/1.282	2006 i
KNCOC → ENCOC (RNCOC)	1.493/1.272	2156 i	1.375/1.281	2005 i
K → C_6H_5CO + CH_3 (RD1)			2.118	402 i
K → C_6H_5 + $COCH_3$ (RD2)			2.165	268 i

Table 2 The reaction enthalpies at 298 K (ΔH_{298}^{0}), the potential barrier heights TSs (ΔE^{TS}) with zero-point energy (ZPE) corrections, relative margin of energies (ΔE^{T1-S0}) between S_0 with T_1 states for the keto-tautomer of acetophenone and its analogues, as well as that of the two C–C bond cleavage reactions, calculated at the B3LYP/6-311+G(d,p) and QCISD(T)/6-311+G(3df,2p)//B3LYP/6-311+G(d,p) levels, respectively (unit in kcal mol^{-1})

ab.	Molecular formula	B3LYP/6-311+G(d,p)				
		ΔE^{S0TS}+ZPE	$\Delta^{S0} H_{298}^{0}$	ΔE^{T1TS}+ZPE	$\Delta^{T1} H_{298}^{0}$	ΔE^{T1-S0}+ZPE
K	(structure: acetophenone)	62.31	13.81	28.71	-1.86	67.07
KC	(structure: 4-methylacetophenone)	62.06	14.20	28.73	-1.86	67.68
KCC	(structure: 4-ethylacetophenone)	62.10	14.32	28.80	-1.80	67.81
p-KP4	(structure: 4-butylacetophenone)	62.15	14.25	28.75	-1.81	67.74
p-KP6	(structure: 4-hexylacetophenone)	62.16	14.19	28.89	-1.77	67.63
p-KP8	(structure: 4-octylacetophenone)	62.04	14.20	28.82	-1.80	69.85
p-KP10	(structure: 4-decylacetophenone)	62.11	14.20	29.01	-1.79	70.01
KN	(structure: 4-aminoacetophenone, NH$_2$)	61.17	15.44	27.89	-2.68	70.56
KNC	(structure: 4-methylaminoacetophenone)	60.87	15.59	35.41	4.41	63.51
KNCOC	(structure: 4-acetamidoacetophenone)	61.81	14.18	30.55	-0.21	65.78
KOH	(structure: 4-hydroxyacetophenone, OH)	61.77	14.69	28.97	-1.73	68.58
KOC	(structure: 4-methoxyacetophenone, O)	61.71	14.88	29.30	-1.35	68.48
KSH	(structure: 4-mercaptoacetophenone, SH)	62.05	14.18	31.37	0.57	64.68
K1	(structure: benzamide, H$_2$N)	42.21	13.12	30.94	7.21	75.92
K2	(structure: benzoic acid, HO)	32.05	0.00	32.16	0.00	74.82
		QCISD(T)/6-311+G(3df,2p)//B3LYP/6-311+G(d,p)				
K→ C$_6$H$_5$CO + CH$_3$ (RD1)				17.92 (19.79)	7.80 (9.28)	
K→ C$_6$H$_5$ + COCH$_3$ (RD2)				27.58 (27.28)	24.99 (21.36)	

[a] experimental value taken from Ref.[8]

that the QCISD(T)/6-311+G(3df,2p)//B3LYP/6-311+G(d,p) level is reasonable and reliable for the studies of the two C–C bond cleavage reactions. Due to the lack of the fully optimized transition states for the two C–C bond cleavage reactions, our calculation may provide reliable information for future experiment investigations.

The calculated results in S_0 state show that the reaction energy barrier of keto-enol isomerization, involving

Table 3 The calculated and experimental adiabatic excitation energies (unit in kcal mol^{-1}) of acetophenone in the lowest five electronically excited states (T$_1$, S$_1$, T$_2$, S$_2$, and S$_3$)

K → E (R)	$\Delta E^{\text{S0-S1}}$	$\Delta E^{\text{S0-S2}}$	$\Delta E^{\text{S0-S3}}$	$\Delta E^{\text{T2-S0}}$	$\Delta E^{\text{T1-S0}}$
QCISD(T)//B3LYP					74.92
CIPT2/cc-pVDZ// CASSCF(12,11)/6-31+G*	79.0[d] 78.1[f] (3.39 eV)	103.14[e] (36 074 cm^{-1}) 101.2[f] (4.39 eV)		71.77[e] (25 102 cm^{-1}) 78.7[f] (3.41 eV)	73.07[e] (25 556 cm^{-1}) 72.5[f] (3.14 eV)
Expl.	77.99[a] (27 279 cm^{-1})	101.22[b] (35 402 cm^{-1})	119.21[c] (41 695 cm^{-1})		73.74[a] (25 791 cm^{-1})

[a] Ref.[8]; [b] Ref.[12]; [c] Ref.[27]; [d] Ref.[10] calculated at CASSCF(10,8)/6-31G* level; [e] Ref.[28] calculated at MCSCF(10,9)/6-311G(d,p) level; [f] Ref.[13]

the simulation that acetophenone is bond linked to the carbon chain para-position of PE, KCC and p-KPn (n = 4, 6, 8, and 10), will decrease, as alkyl groups will exhibit inductive electron-donating effect and σ-π super-conjugated effect. As a result, a lower amount of energy is needed to complete the keto-enol isomerization, which is much lower than that for the carbon-carbon single bond energy (average bond energy is 82.95 kcal mol^{-1}) in XLPE. We replaced the –CH$_3$ in the acetyl group of acetophenone by –NH$_2$ (K1) or –OH (K2). The H in –NH$_2$ and –OH will be more active than that in –CH$_3$ due to the larger electronegativity of N and O than that of C. Therefore, the H in –NH$_2$ and –OH dissociates easier and leads to more facile isomerization and lower energy barriers.

When heteroatom (N, O, and S) is linked to acetonpheone via single bond in S$_0$ state, the energy barriers of keto-enol isomerization will be decreased. Distinct electron donating conjugated effect and relatively weak electron withdrawing inductive effect will be present when –NHR (R = H, CH$_3$, and CH$_2$CH$_3$) is linked to benzene ring (KN, KNC, and KNCC). The electron withdrawing effect is larger when the substituent group is acylamino (KNCOC) than KN, the energy barrier is still lower than K. When –OR and –OH links to acetonpheone, they exhibit inductive electron withdrawing effect and electron donating conjugated effect at the same time, while the latter is stronger than the former and results in good electron donating effect at last. The electron density in benzene ring will be increased when electron-donating group links to acetonpheone, and it will further impel the transfer of π electrons to O in –C = O, which will in turn exert stronger attraction to H in acetyl, and thus isomerization occurs in an easier fashion. In the case of KSH in S$_0$ state, S and O belong to the same oxygenic group and possess similar electron effect. Moreover S has a larger atomic radius and conjugate less efficiently to benzene ring than O. Hence, energy barrier of isomerization decreases to a lesser extent than that of –OH, when –SH links to the para-position of acetonpheone. C, N, and O all belong to the same second period of element, and follow an electron-donating capability order of –NH$_2$ > –OH > −R. When N, O, and C atoms are linked to para-position of acetonphenone (KN, KOH, and KC), the corresponding energy barriers of isomerization will gradually increase accordingly as the order shown in the Table 2.

The above results indicate that the better electron donating ability of groups linked to acetophenone, the more energy barrier decreases, the easier isomerization occurs, the easier the energy high-energy electrons absorbed and transferred when high-energy electrons are injected into PE, without reference to acetophenone and its analogues are doped into or acetophenone bonded to the chains of PE, and vice versa. The conjugation in acetophenone between the aromatic ring and the carbonyl group has a noticeable influence on the relative energies of the nπ* and ππ* states as well as their chemical reactivity. Upon energies of high-energy electronics absorption, acetophenone can undergo two general types of processes: isomerization and transitions between electronic states while either conserving spin (internal conversion) or altering spin (intersystem crossing). When acetophenone absorbs the energy, it is initially excited to the bright S$_2$ state (adiabatic excitation energy 101.22 [27] kcal mol^{-1}), followed by an ultrafast S$_2$ → S$_1$ internal conversion and relaxation to the S$_1$ minimum (77.99 [8] kcal mol^{-1}). The S$_1$ → T$_1$ intersystem crossing can occur efficiently. With the available excess energy, acetophenone can overcome the barriers of cleavage in the T$_1$ state (RD1 at 17.92 kcal mol^{-1} and RD2 at 27.58 kcal mol^{-1}) and form the corresponding ground-state products. With the rather small TS energy barrier of dissociation channel, RD1 is expected to be accessible with a preference cleavage for forming C$_6$H$_5$CO and CH$_3$ radicals.

When the electron energy accumulated by electric field exceeds 62.31 kcal mol^{-1}, acetophenone exchanges the energy with this "hot" electron, accomplishes isomerization from keto- to enol-tautomers, and releases a secondary electron with low energy. When the system absorbs energy from another "hot" electron, isomerization reaction from enol- to keto-tautomers occurs. The reaction occurs repeated made the "hot" electrons "cool" which cannot bob the C-C bond of XLPE with 82.95 kcal mol^{-1} bond breaking energy. With the macro-point of view, the composite exhibits an elevated initiation voltage of electrical tree and AC breakdown strength.

The detailed knowledge of mechanism for aromatic carbonyl compounds provides the basis for our understanding of the chemical compound doping or bond linked with XLPE electrical properties improvement. Looking further into the future, theoretical calculations provide not only new insights

into experimental findings but also some guidance to experimental study of mechanism of elevating breakdown strength of XLPE. The relative work is currently underway. Further work to account for electron flux during the chemical reaction [29, 30], intramolecular stabilization effects QTAIM analysis [31–34], ionization potentials, electron affinities, extraction potentials, and reorganization energies etc. in a selected set of the presently investigated molecules additive in XLPE is under way.

Conclusions

In this paper, a systematically theoretical study on the mechanism of isomerizations of acetophenone and its analogues in S_0 and T_1 states and the two C–C bond fission reactions have been carried out. On S_0 state, energy barriers for these isomerization reactions (30 reaction systems) are needed to overcome for both reactions of keto- to enol- and enol- to keto-tautomers. The energy barriers of isomerization from keto- to enol-tautomers decrease when electron donating alkyl groups or heteroatoms are linked to para-position of acetophenone. The energy barriers obviously decrease in T_1 triplet state versus its S_0 ground state. To overcome energy barriers of both forward and reverse reactions are almost equal in the T_1 state. The cleavage is strongly dominant of dissociation channel RD1 because of the lower barrier. The energy barriers of the 30 reactions are lower than that for the breakdown of the C-C single bond in XLPE. Finally, acetophenone can inhibit polyethylene electrical tree as well as improve the alternate breakdown strength XLPE through either doping into PE composite or linked to PE chains.

References

1. Liao RJ, Zheng SX, Yang LJ, Liu L, Ye KY (2010) High Voltage Eng 36(10):2398–2404
2. Zheng XQ, Chen G, Davies AE (2003) Adv Technol Electr Eng Energy 22(4):21–24
3. Sekii Y, Tanaka D, Saito M, Chizuwa N, Kanasawa K (2003) Annual Report Conference on Electrical Insulation and Dielectric Phenomena pp66–665
4. Sarathi R, Das S, Venkataseshaiah C, Yoshimura N (2003) Annual Report Conference on Electrical Insulation and Dielectric Phenomena pp666–669
5. Tu DM, Wu LH, Wu XZ, Chong SK (1981) J Xi'an Jiaotong Univ 15(2):95–106
6. Yamano Y, Iizuka M (2009) IEEE Trans Dielectr Electr Insul 16(1):189–198
7. Englund V, Huuva R, Gubanski SM (2009) IEEE Trans Dielectr Electr Insul 16(5):1455–1460
8. Ohmori N, Suzuki T, Ito M (1988) Why does intersystem crossing occur in isolated molecules of benzaldehyde, acetophenone, and benzophenone? J Phys Chem 92:1086–1093
9. Fang WH (2008) Ab initio determination of dark structures in radiationless transitions for aromatic carbonyl compounds. Acc Chem Res 41(3):452–457
10. Fang WH, Phillips DL (2002) The Crucial Role of the $S_1/T_2/T_1$ Intersection in the relaxation dynamics of aromatic carbonyl compounds upon n → π* excitation. ChemPhysChem 10:889–892
11. Feenstra JS, Park ST, Zewail AH (2005) Excited state molecular structures and reactions directly determined by ultrafast electron diffraction. J Chem Phys 123:221104
12. Park ST, Feenstra JS, Zewail AH (2006) Ultrafast electron diffraction: excited state structures and chemistries of aromatic carbonyls. J Chem Phys 124:174707
13. Cui GL, Lu Y, Thiel W (2012) Electronic excitation energies, three-state intersections, and photodissociation mechanisms of benzaldehyde and acetophenone. Chem Phys Lett 537:21–26
14. Li J, Zhang F, Fang WH (2005) Probing photophysical and photochemical processes of benzoic acid from ab initio calculations. J Phys Chem A 109:7718–7724
15. Fang Q, Liu YJ (2010) Wavelength-dependent photodissociation of benzoic acid monomer in α C-O fission. J Phys Chem A 114:680–684
16. Zhao HQ, Cheung YS, Liao CL, Liao CX, Ng CY, Li WK (1997) A laser photofragmentation time-of-flight mass-spectrometrometric study of acetophenone at 193 and 248 nm. J Chem Phys 107(18):7230–7241
17. Rubio-Pons Ó, Loboda O, Minaev B, Schimmelpfennig B, Vahtras O, Ågren H (2003) CASSCF calculations of triplet-state properties. Applications to benzene derivatives. Mol Phys: Int J Interface Between Chem Phys 101:2103–2114
18. Minaev BF, Knuts S, Ågren H, Vahtras O (1993) The vibronically induced phosporescence in benzene. Chem Phys 175:245–254
19. Parr RG, Yang W (1989) Density-functional theory of atoms and molecules. Oxford University Press, New York, pp 47–69
20. Truong TN, Duncan WT, Bell RL (1996) Chemical applications of density-functional theory. American Chemical Society, Washington, DC, p85
21. Lee C, Yang W, Parr RG (1988) Phys Rev B 37:785–789
22. Miehlich B, Savin A, Stoll H, Preuss H (1989) Chem Phys Lett 157:200–206
23. Becke AD (1993) J Chem Phys 98:5648–5652
24. Pople JA, Head-Gordon M, Raghavachari K (1987) Quadratic configuration interaction. A general technique for determining electron correlation energies. J Chem Phys 87:5968–5975
25. Frisch MJ, Trucks GW, Schlegel HB, Scuseria GE, Robb MA, Cheeseman JR, Scalmani G, Barone V, Mennucci B, Petersson GA, Nakatsuji H, Caricato M, Li X, Hratchian HP, Izmaylov AF, Bloino J, Zheng G, Sonnenberg JL, Hada M, Ehara M, Toyota K, Fukuda R, Hasegawa J, Ishida M, Nakajima T, Honda Y, Kitao O, Nakai H, Vreven T, Montgomery JA, Jr, Peralta JE, Ogliaro F, Bearpark M, Heyd JJ, Brothers E, Kudin KN, Staroverov VN, Kobayashi R, Normand J, Raghavachari K, Rendell A, Burant JC, Iyengar SS,

Tomasi J, Cossi M, Rega N, Millam JM, Klene M, Knox JE, Cross JB, Bakken V, Adamo C, Jaramillo J, Gomperts R, Stratmann RE, Yazyev O, Austin AJ, Cammi R, Pomelli C, Ochterski JW, Martin RL, Morokuma K, Zakrzewski VG, Voth GA, Salvador P, Dannenberg JJ, Dapprich S, Daniels AD, Farkas O, Foresman JB, Ortiz JV, Cioslowski J, Fox DJ (2009) Gaussian Inc, Revision A.02, Wallingford, CT

26. Hammond GS (1955) J Am Chem Soc 77:334–338
27. Warren JA, Bernstein ER (1986) The S2 ← S0 laser photoexcitation spectrum and excited state dynamics of jet-cooled acetophenone. J Chem Phys 85:2365
28. Leopold DG, Hemley RJ, Vaida V (1981) J Chem Phys 75:4758
29. Gómez S, Guerra D, López JG, Toro-Labbé A, Restrepo A (2013) A detailed look at the reaction mechanisms of substituted carbenes with water. J Phys Chem A 117:1991–1999
30. Herrera B, Toro-Labbe A (2007) The role of reaction force and chemical potential in characterizing the mechanism of double proton transfer in the adenine-uracil complex. J Phys Chem A 111:5921–5926
31. Baryshnikov GV, Minaev BF, Minaeva VA, Podgornaya AT, Ågren H (2012) Application of Bader's atoms in molecules theory to the description of coordination bonds in the complex compounds of Ca^{2+} and Mg^{2+} with methylidene rhodanine and its anion. Rus J Gen Chem 82:1254–1262
32. Baryshnikov GV, Minaev BF, Minaeva VA (2011) Theoretical study of the models of Ca^{2+} and Mg^{2+} ions binding by the methylidene rhodanine neutral and anionic forms. Russ J Gen Chem 81:576–585
33. Baryshnikov GV, Minaev BF, Minaeva VA, Podgornaya AT (2012) Theoretical study of the dimerization of rhodanine in various tautomeric forms. Chem Heterocycl Compd 47:1268–1279
34. Baryshnikov GV, Minaev BF, Minaeva VA, Ågren H (2010) Theoretical study of the conformational structure and thermodynamic properties of 5-(4-oxo-1,3-thiazolidine-2-ylidene)-rhodanine and ethyl-5-(4-oxo-1,3-thiazolidine-2-ylidene)-rhodanine-3-acetic acid as acceptor groups of indoline dyes. J Struct Chem 51:817–823